J Shoulder Elbow Surg (2020) 29, 2395–2405

ELSEVIER

Journal of Shoulder and Elbow Surgery

www.elsevier.com/locate/ymse

Influence of implant design and parasagittal acromial morphology on acromial and scapular spine strain after reverse total shoulder arthroplasty: a cadaveric and computer-based biomechanical analysis

Sarav S. Shah, MD[a,*], Joseph Gentile, MD[b], Xiang Chen, MS[c], Andreas Kontaxis, PhD[c], David M. Dines, MD[c], Russell F. Warren, MD[c], Samuel A. Taylor, MD[c], Amirhossein Jahandar, MS[c], Lawrence V. Gulotta, MD[c]

[a]*Division of Sports Medicine, Department of Orthopaedic Surgery, New England Baptist Hospital, Boston, MA, USA*
[b]*Department of Orthopaedic Surgery, Novant Health, Huntersville, NC, USA*
[c]*Shoulder and Elbow Division of the Sports Medicine Institute, Hospital for Special Surgery, New York, NY, USA*

Background: The purpose was to analyze the influence of deltoid lengthening due to different implant designs and anatomic variations of the acromion and scapular spine (SS) in the parasagittal plane on strain patterns after reverse shoulder arthroplasty (RSA).
Methods: Ten cadaveric shoulders with strain rosettes placed on the surface of the acromial body (Levy II) and SS (Levy III) were tested using a shoulder simulator. RSA using humeral onlay (+3, +5, +8, +10, +13 mm) and glenosphere lateralization (0, +6 mm) was performed. Arm lengthening and magnitude of strain on acromion/SS were measured. The length of deltoid was assessed using validated computer modeling. Anatomic variance of the SS angle and position of acromion in relation to the scapular plane was examined. For comparison of strain as a function of deltoid lengthening, 25 mm was used as a threshold value for comparison based on previous literature demonstrating a decrease in Constant score and active anterior elevation in patients with arm lengthening >25 mm.
Results: At maximal deltoid lengthening (30.8 mm), average strains were 1112 με (acromion) and 1165 με (SS) ($P < .01$). There was an 82.6% increase in acromial strain at maximum lengthening compared with 25 mm ($P = .02$) and a strain increase of 79 με/mm deltoid lengthening above a threshold of 25 mm. The strain results delineated 2 anatomic groups: 5 of 10 specimens (group A) showed higher strain on SS (1445 με) vs. acromion (862 με, $P = .02$). Group A had a more posteriorly oriented acromion, whereas group B was anteriorly oriented ($P < .001$).
Conclusion: Deltoid lengthening above 25 mm produced large strains on the acromion/SS. Anatomic variation may indicate that as the acromion is more posteriorly oriented, the SS takes more strain from the deltoid vs. the acromion. Our study's data may help surgeons identify a high-risk population for increased strain patterns after RSA.
Level of evidence: Basic Science Study; Biomechanics

Keywords: Reverse shoulder arthroplasty (RSA); acromial fracture; scapular spine fracture; anatomic variation; strain

Acromial stress fractures (AF) are a relatively common complication after RSA. In a recent study, Patterson et al[18] reported an AF and scapular spine fracture (SSF) rate of 4.4% in their systematic review of 3838 RSAs. AF and

Approval was obtained from the Hospital for Special Surgery Institutional Review Board.

*Reprint requests: Sarav S. Shah, MD, New England Baptist Hospital, 125 Parker Hill Avenue, Boston, MA 02120, USA.
E-mail address: saravshah1@gmail.com (S.S. Shah).

1058-2746/$ - see front matter © 2020 Journal of Shoulder and Elbow Surgery Board of Trustees. All rights reserved.
https://doi.org/10.1016/j.jse.2020.04.004

SSFs can be difficult to classify; 2 classification schemes have been described in the literature.[5,13] Crosby et al[5] described fractures based on their location relative to the acromioclavicular joint. In their study, they reported an overall fracture rate of 5.5% after RSA. Type I fractures are an avulsion of the anterior acromion, type II fractures occur posterior to the acromioclavicular joint, and type III fractures are those of the scapular spine (SS). Levy et al[13] classified scapular fractures after RSA based on their relation to the deltoid insertion. Type I fractures involved a portion of the anterior and middle deltoid. Type II included the entire meddle deltoid with a portion of the posterior deltoid. Type III fractures included the entire middle and posterior deltoid origins.

Importantly, AF and SSFs can be very difficult to treat;[15] Levy type I fractures have shown good results with conservative treatment, whereas the treatment of Levy type II and III fractures is still controversial. Immobilization with an abduction splint may result in nonunion or malunion,[16] and operative intervention may not improve overall outcomes.[15] SSFs (Levy type III)[13] pose a unique challenge. A vast amount of deltoid origin is involved with this fracture type; thus there is a heighted concern for nonfunctional deltoid musculature accompanying a potential malunion/nonunion.[15] Operative management has been recommended. Regardless of treatment, patients who sustained postoperative acromial and SS fractures report inferior function compared with initially after RSA,[18] and final clinical outcomes scores are reduced compared with patients after RSA without scapular fracture.[2,16,18,24]

The exact biomechanical mechanism for the increased strain patterns that are thought to be associated with AF/SSF after RSA remains undefined. Some authors have theorized that excessive tensioning of the deltoid after RSA causes significant strain on the acromion secondary to disproportionate lowering of the humerus leading to arm lengthening.[7,13,28] Others have suggested that glenosphere lateralization causes increased strain that may lead to AF secondary to an increase in the required deltoid abduction force.[10,11] The proposed clinical risk factors for AF and SSF include osteoporosis,[17,28] and furthermore, the varied incidences of different types of acromial fractures may indicate an association with patients' premorbid bony anatomy of the acromion and the SS.

Thus, the primary purpose of this cadaveric study was to quantify a relationship between deltoid lengthening using implant variation (humeral onlay polyethylene thickness and glenosphere lateralization) in a 147° neck-shaft angle implant and a 36-mm glenosphere with acromion/SS strain patterns after RSA. A secondary purpose was to investigate if there is anatomic variance of the acromion/SS that may play a role in strain patterns after RSA. For comparison of strain as a function of deltoid lengthening, 25 mm was used as a threshold value for comparison based on previous literature demonstrating a decrease in Constant score and active anterior elevation in patients with arm lengthening >25 mm. Our main hypothesis was that there would be a large increase in strain patterns on both the acromion and SS with deltoid lengthening above 25 mm. We also hypothesized that increased parasagittal humeral coverage of the acromion would increase SS strains after RSA.

Materials and methods

This is a cadaveric and computer-based biomechanical analysis study. Ten cadaveric shoulders (8 male, 2 female) with an average age of 53.2 (range, 37-63; standard deviation [SD], 9.1) years and an average body mass index of 39.1 (range, 34-44; SD, 3.8) were tested using an established custom 6-degree-of-freedom shoulder simulator (Fig. 1).[26] None of the specimens showed any macroscopic or radiological signs of acromial, SS or glenohumeral pathologies or anomalies. Strain rosettes were placed on to the surface of the acromial body (A) and SS. The effects of 2 implant parameters, humeral onlay polyethylene thickness (+3, +5, +8, +10, +13 mm) and glenosphere lateralization (0 and +6 mm lateralized), were assessed for 2 outcomes: (i) the amount of arm lengthening (humeral distalization) and (ii) the magnitude of maximal principal strain on the acromion and SS. Deltoid lengthening was calculated using the measured arm positioning data and computer modeling (OpenSim) that calculated the wrapping of the muscle. Anatomic variance of the specimens was determined with regard to the angle of the SS to the scapular plane (scapular spine angle [SSA]) and the position of the acromion in relation to the scapular plane (Fig. 2). With the advent and widespread utilization of 3D planning for shoulder arthroplasty, the SSA and parasagittal orientation of the acromion were selected as simple tools that a surgeon could use during preoperative planning.

Specimen preparation

The entire shoulder girdle including scapula, clavicle, and humerus from 10 fresh frozen cadavers were dissected of all skin and soft tissues with the exception of the deltoid. The scapulae and humeri of the 10 specimens were instrumented with optical motion capture marker clusters. A pretesting 3D computed tomography (CT) was performed for each specimen to register the bony geometries to the marker clusters so that a 4-camera motion analysis system (Motion Analysis Corporation, Santa Rosa, CA, USA) could record the position and motion of the shoulder segments with an accuracy of 0.1 mm.

Strain rosettes (Vishay Measurements Group, Raleigh, NC, USA), 3 strain gauges overlapping and patterned in a 90° angle, were rigidly glued on to the surface of the acromial body and SS to represent the locations of Levy et al[13] type II and type III fractures, respectively (Fig. 1). Bony surfaces of the acromial body and SS were carefully prepared to remove all the attached soft tissues and periosteum, and ensure the full exposure of the cortical bone. The bony surface was degreased using an acetone-based agent before applying the strain rosettes. Each strain rosette measured surface strains on the bone in 3 directions (following the directions of the 90° patterned 3 single strain gauges), and therefore allowed the calculation of the principal strains that are immaterial to the direction of each single strain gauge in the rosette.

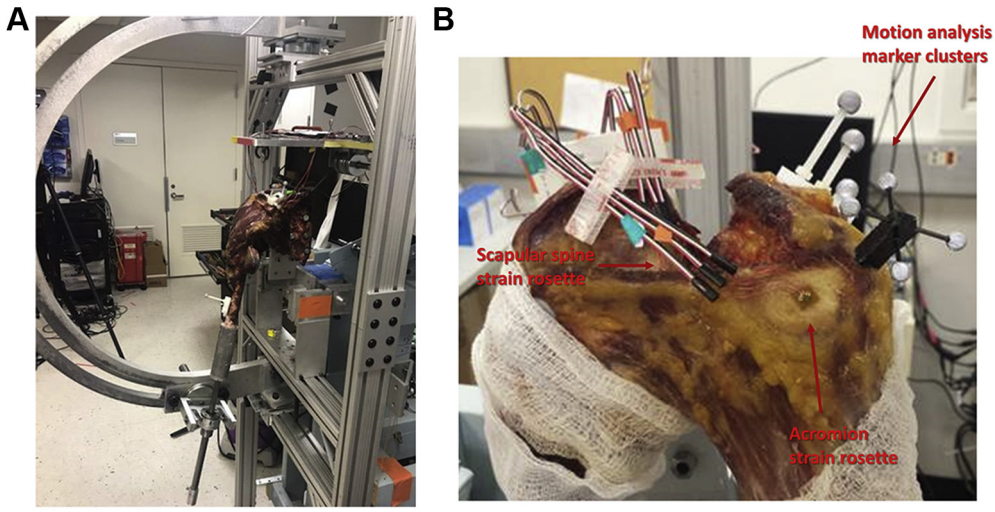

Figure 1 Biomechanical testing apparatus. (**A**) The humerus was mounted to a 6-degree-of-freedom shoulder simulator that can simulate different levels of abduction. (**B**) Strain rosettes (Vishay Measurements Group), 3 strain gauges overlapping and patterned in a 90° angle, were rigidly glued on to the surface of the acromial body and the scapular spine to represent the locations of Levy et al type II and type III fractures, respectively.

The scapula of each specimen was rigidly fixed to a custom scapula fixation device using a minimum of 3 heavy duty metal screws. The custom scapula fixation device allows the adjustment of scapula orientations in scapula abduction and tilt before fixation. The humeral shaft was then potted into a 5 by 1.5-inch aluminum cylinder with poly(methyl methacrylate) cement. The aluminum cylinder was rigidly connected to a metal shaft and mounted to a 6-degree-of-freedom shoulder simulator (Fig. 1).

Before mechanical testing and RSA implantation and for each specimen, the positions of the landmarks of the most distal point of the deltoid humeral insertion on the deltoid tuberosity and the most anterior and posterior points of the deltoid origin on the acromion and the SS were identified on the CT scans. The landmarks were registered to a humeral and scapular cluster of retroreflective markers (also visible on the CT). The clusters that were tracked by the motion system ensured high-fidelity position tracking. The data were then used in a cadaver-specific computer shoulder model (OpenSim) that calculated the wrapping of the muscle.

Measurements of anatomic variance between specimens

The SSA

The angle of the SS relative to the scapular plane was defined as the SSA. This angle was used to describe the relative geometry of the SS and the parasagittal humeral coverage or ''overhang'' of the acromion (Fig. 2). The scapular plane was defined for each specimen using 3 bony landmarks: center of the glenoid, most medial point of the SS, and the inferior angle of the scapula. The center of the glenoid was defined as the projected intersection of the superior inferior axis and the anterior-posterior axis (at the widest margins of the glenoid rim). This was located on average at a location one-third the length of the superior-inferior axis from the inferior border of the glenoid. The SSA was measured in a cross-sectional 2D CT plane that is perpendicular to the scapular plane. In the cross-sectional 2D CT plane, a line was drawn to bisect the bony region of the SS. Using the cross-sectional 2D CT and 3D reconstruction, the SSA was measured as the angle between the newly drawn line and the scapular plane (Fig. 3A). The medial-lateral position of this cross-sectional plane was chosen as the position where the strain rosette was glued on the SS, which was approximately 0.5 cm medial to the spinoglenoid notch. The medial-lateral distance between the strain gauge and the spinoglenoid notch was consistent across all the specimens (0.5 ± 0.4 cm).

Acromion extension

For each specimen, the most anterior point of the acromion was identified in a plane that is parallel to the scapular plane. The anterior/posterior extension of the acromion was calculated as the perpendicular distance from the most anterior point of the acromion to the point parallel to the center of the glenoid in the scapular plane (Fig. 3B). The anterior extension of the acromion (the most anterior point of the acromion lay anteriorly to the scapular plane) was denoted in positive (+) values, whereas posterior extension was denoted in negative (−).

Reverse shoulder arthroplasty implantation: arm lengthening and strain measurements

RSA was implanted in each specimen using a 147° neck-shaft angle implant with a 36-mm glenosphere and humeral

Figure 2 The angle of the scapular spine relative to the scapular plane was defined as the scapular spine angle. This angle was used to describe the relative geometry of the scapular spine. The scapular plane was defined for each specimen using 3 bony landmarks: center of the glenoid, most medial point of the scapular spine, and the inferior angle of the scapula.

onlay component (Zimmer Biomet Comprehensive Reverse Shoulder System, Warsaw, IN, USA). For each specimen, RSA was implanted using standard instrumentation by a single orthopedic fellowship trained surgeon following a standardized surgical protocol. For each specimen, the humeral head was resected at the anatomic neck, with the humeral component aligned to the native humeral version. For each specimen, the base plate combined with a central screw and 4 peripheral screws were placed in the same location at the center of the glenoid for implantation with a 36-mm standard glenosphere in a concentric location. Postoperative CT scan was used to ensure accurate superior screw tracks in all specimens.

The effects of 2 implant parameters, humeral onlay lateralization, with humeral tray and polyethylene thickness (+3, +5, +8, +10, +13 mm), and glenosphere lateralization (0 and +6 mm lateralized), were assessed for 2 outcomes: amount of arm lengthening (humeral distalization) and magnitude of maximal principal strain on the acromion and SS. The humerus was positioned at 0 glenohumeral abduction and at 0 glenohumeral rotation as impingement free range of motion allowed. This was assumed as the position of maximum deltoid lengthening. For the 10 test combinations, glenohumeral abduction and rotation angles were maintained, whereas the humerus was free to translate in its axial direction. A 4-camera optical motion capture system (Motion Analysis Corporation) was used to track the marker clusters that were attached to the bony segments with a residual error of 0.1 mm. This allowed calculating the change of positions of the humerus with the different combinations of glenosphere and humeral onlay lateralization to determine the amount of arm lengthening. Strains on the acromial body and SS were recorded using Labview (National Instruments, Austin, TX, USA). The acquired strain signals were synchronized with the motion capture system.

Evaluation of deltoid lengthening

Although prior clinical studies have used radiographic arm lengthening, it may not be the most accurate surrogate for deltoid lengthening. It is dependent on multiple factors[14] and has a self-reported large SD (−23 to 52 mm).[27] The calculation of deltoid lengthening in our study was performed using a validated computer model and may be a more accurate delineation as the simulation of 5 deltoid fibers more accurately follows the line of action of the deltoid.

To avoid metal artifact, the implant components were removed after mechanical testing before conducting a postoperative CT scan. However, before removal, the position of the implants was registered in relation to the bones with the motion capture and a marker pointer. The 3D models of the postoperative scapulae and humeri were reconstructed, and a virtual RSA implantation was performed using a 3D model of the prosthesis that was used in the experiment. Accurate placement and alignment of the prosthesis on the model was achieved by using the postoperative CT scans of the cadavers and the registration data of implants to the bones. After the virtual implantation, a 3D post-RSA shoulder model was generated for each specimen in OpenSim software. The attachment and origins of the deltoid muscle fibers were transferred from the pre-RSA shoulder model to the post-RSA model. In OpenSim, the humerus was then aligned to the humeral adduction position according to the glenohumeral angles recorded by the motion capture system during the testing. By changing the 3D geometries of the glenosphere and the humeral insert in the post-RSA shoulder model, whereas maintaining the glenohumeral rotations at

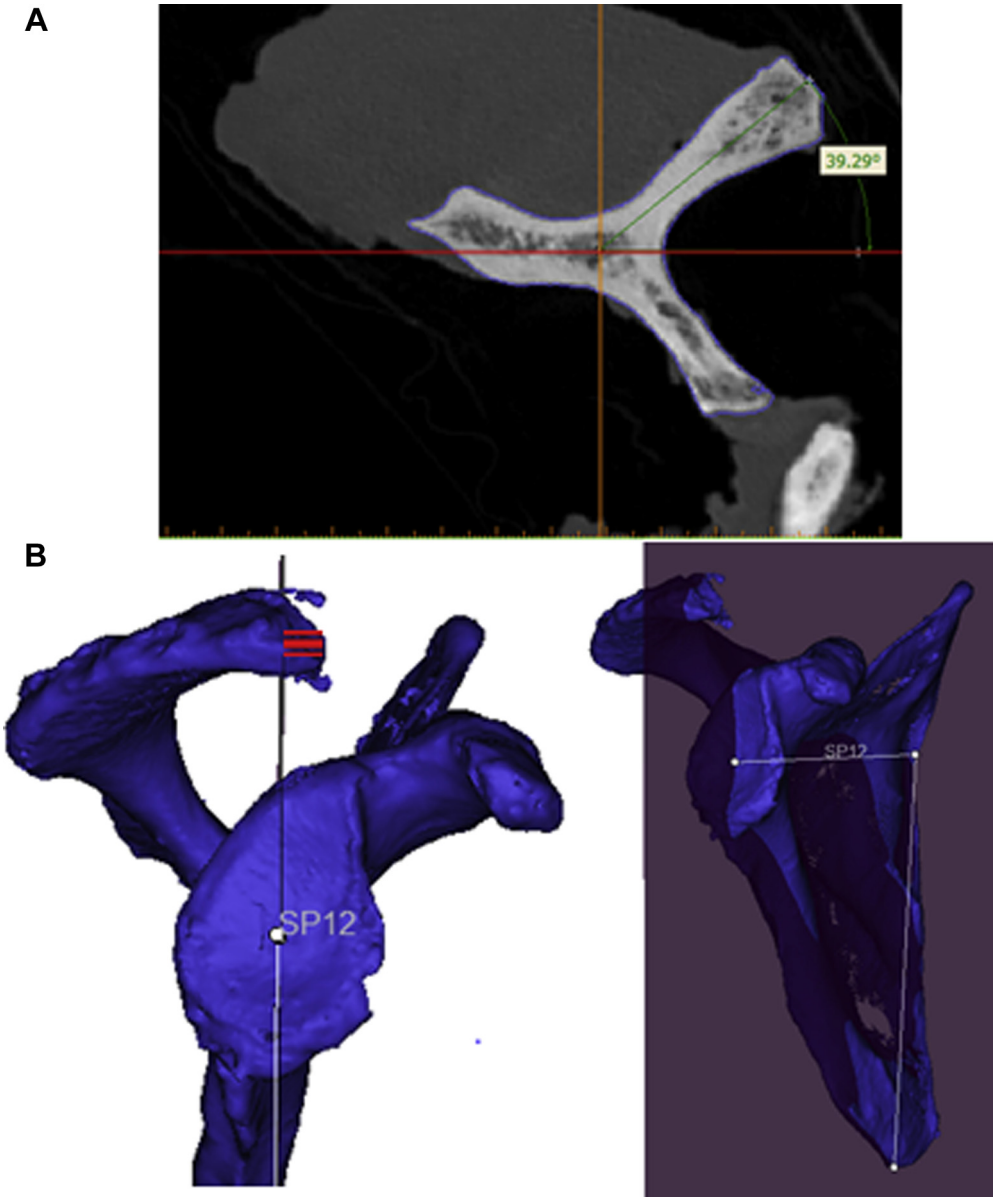

Figure 3 (**A**) Scapular spine angle (SSA) measurement. In the cross-sectional 2D computed tomography plane, a line was drawn to bisect the bony region of the scapular spine. The SSA was measured as the angle between the newly drawn line and the scapular plane. (**B**) Acromion extension. The most anterior point of the acromion was identified in a plane that is parallel to the scapular plane. The anterior/posterior extension of the acromion was defined as the perpendicular distance from the most anterior point of the acromion to the scapular plane. The anterior extension of the acromion (the most anterior point of the acromion lay anteriorly to the scapular plane) was denoted in positive values, whereas posterior extension was denoted in negative values.

the tested humerus adduction, the lengths of the deltoid fibers were calculated for different combinations of glenospheres and humeral inserts. For each specimen, the post-RSA deltoid lengths were normalized to the deltoid lengths measured in the pre-RSA intact shoulder model at the same adduction position. The shoulder model represents muscles as non-frictional elastic strings that wrap around bony geometries.[4] This method of muscle modeling has been validated for muscle moment arms and lengths against cadaveric models by multiple studies.[1,8,9]

Statistical analysis

Repeated measures analysis of variance with post hoc Bonferroni analysis was used to determine differences in maximum principal strain for the acromion and SS across different combinations as well as to determine differences in anatomic variation between the specimens. Furthermore, a linear regression model was determined for both acromial and SS strain based on deltoid lengthening. An alpha value less than 0.05 was considered statistically significant. For

comparison of strain as a function of deltoid lengthening, 25 mm was used as a threshold value for comparison based on Werner et al,[27] who observed a decrease in Constant score and active anterior elevation in patients with arm lengthening >25 mm vs. patients with 10-25 mm.

Results

Arm lengthening and deltoid lengthening measurements

For the 10 cadavers tested, each increment of humeral onlay lateralization had an increase of arm lengthening (from 18.4 ± 3.3 mm with the standard humeral insert to 28.8 ± 3.4 mm with the +13 insert using the standard offset glenosphere, Table I, $P < .001$, for all pairwise comparisons). As glenosphere lateralization would likely affect arm lengthening mostly in the abducted position, it is a notable observation that glenosphere lateralization did not result in a significant change in arm lengthening ($P = .823$).

The calculated length of the deltoid showed that on average, both glenosphere lateralization and humeral insert affected the results. For the standard glenosphere, deltoid lengthening increased from 16.1 ± 4.7 mm with the standard humeral insert to 28.6 ± 4.8 mm with the +13 insert ($P < .01$). The lateralized glenosphere also increased the deltoid lengthening from 18.1 ± 5.0 mm with the standard humeral insert to 30.8 ± 5.0 mm with the +13 insert using the lateralized glenosphere ($P < .01$). Peak deltoid lengthening was seen in the +6 mm lateralized glenosphere with the +13 mm humeral onlay thickness at 30.8 ± 5.0 mm.

Acromion and scapular spine strain measurements

Average maximum principal strains on the acromion increased with each incremental increase of humeral onlay ($P < .05$ for each pairwise comparison). Furthermore, in all humeral onlay conditions, lateralization of the glenosphere further increased the strain on the acromion, but differences were only significant for the +10 and +13 mm onlay inserts ($P = .029$ and $P = .048$, respectively).

For both the standard and lateralized glenosphere, there was a significant ($P = .011$) linear correlation between acromial strain and deltoid lengthening with a high correlation value ($R^2 = 0.979$ and $R^2 = 0.996$ for standard and +6 glenosphere, respectively) (Fig. 4). At maximal deltoid lengthening, the average maximal principal strain of 1112 ± 366 με was seen on the acromion. Of note, there was an 82.6% increase in strain at the maximum deltoid lengthening compared 25 mm lengthening ($P = .021$). Furthermore, there was a maximal principal strain increase of 79

Table I Maximal principal strain for the acromion and scapular spine according to deltoid lengthening with various implant configurations

Passive deltoid lengthening (mm)	Amount of arm lengthening (mm)	Implant configuration (glenosphere lateralization and humeral onlay lateralization)	Max principal strain (average in με): acromion	Max principal strain (average in με): scapular spine
19.0	20.8	Glenosphere 0 mm Humeral onlay +3 mm	348	509
20.9	22.4	Glenosphere 0 mm Humeral onlay +5 mm	427	539
21.0	20.8	Glenosphere +6 mm lateralization Humeral onlay +3 mm	380	544
23.0	22.4	Glenosphere +6 mm lateralization Humeral onlay +5 mm	568	700
23.8	24.8	Glenosphere 0 mm Humeral onlay +8 mm	609	758
25.7	26.4	Glenosphere 0mm Humeral onlay +10 mm	696	805
25.9	24.8	Glenosphere +6 mm lateralization Humeral onlay +8 mm	758	919
27.9	26.5	Glenosphere +6 mm lateralization Humeral onlay +10 mm	905	990
28.6	28.8	Glenosphere 0 mm Humeral onlay +13 mm	962	1059
30.8	28.9	Glenosphere +6 mm lateralization Humeral onlay +13 mm	1112	1165

There was an 82.6% increase in strain at the acromion at the maximum deltoid lengthening compared with 25 mm lengthening ($P = .021$) with a maximal principal strain increase of 79 με/mm deltoid lengthening above a threshold of 25 mm. There was a 43.7% increase in strain at the scapular spine at the maximum deltoid lengthening compared with 25 mm deltoid lengthening ($P < .01$) with a maximal principal strain increase of 66 με/mm deltoid lengthening above a threshold of 25 mm.

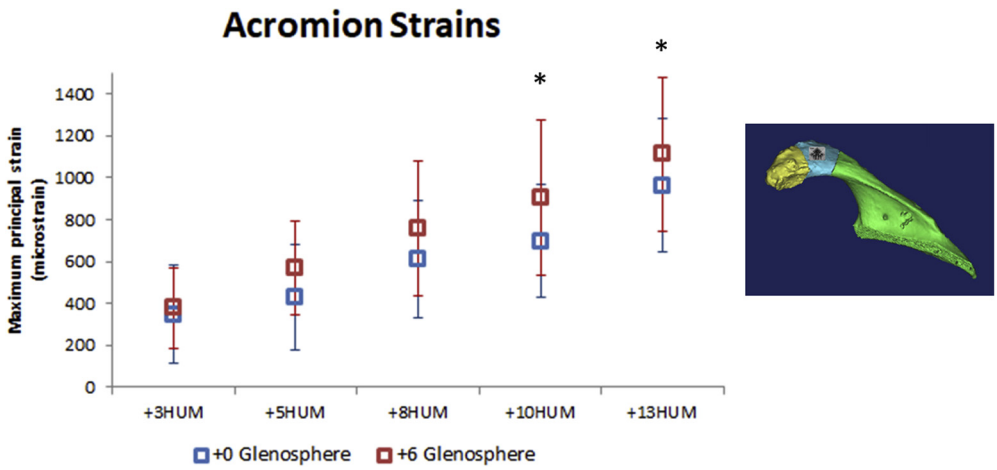

Figure 4 Maximum principal strain on the acromion with different implant configurations. Lateralization of the glenosphere further increases the strain on the acromion with increasing humeral onlay thickness. *Indicates a significant difference between standard and lateralized glenospheres.

με per mm deltoid lengthening above a threshold of 25 mm (Table I).

Similarly, the maximum principal strain patterns on the SS are linear with both the standard glenosphere and the +6 mm lateralized glenosphere (Fig. 5, $P < .01$, $R^2 = 0.963$ and $R^2 = 0.987$ for standard and +6 mm glenosphere, respectively). At maximal deltoid tension, the average principal strain of 1165 ± 719 με was seen on the SS. Of note, there was a 43.7% increase in strain at the maximum deltoid lengthening compared with 25 mm deltoid lengthening ($P < .01$). Furthermore, there was a maximal principal strain increase of 66 με/mm deltoid lengthening above a threshold of 25 mm (Table I).

Anatomic variance of the specimens

The strain results divided the cadavers into 2 groups. These strain patterns were observed in all tested implant configurations for specimens in the different groups ($P < .01$ for each pairwise comparison). At the maximum deltoid lengthening (adduction using the +6 mm lateralized glenosphere and +13 humeral onlay), 5 of 10 specimens (group A) showed higher strain on the SS (1445 ± 655 με) compared with strain on the acromion (862 ± 323 με, $P = .020$; Fig. 5). In contrast, the other 5 specimens (group B) showed higher strain on the acromion (1203 ± 211 με) compared with strain on the SS (603 ± 173 με, $P = .003$). Group A had a larger mean SSA (55 ± 2°) compared with group B (42 ± 3°, $P < .001$). On average, specimens in group A correspondingly had a more posteriorly oriented acromion (−5.3 ± 3.4 mm, acromion is posterior relative to the scapular plane), whereas group B had an anteriorly oriented acromion (6.7 ± 1.6 mm, $P < .001$) (Fig. 6).

Discussion

Based on the results of this study, increased deltoid lengthening via humeral onlay and glenosphere lateralization corresponds with increased strain on the acromion and SS, particularly above 25 mm. Acromial strain at maximal deltoid tension (+13 mm humeral onlay and +6 mm lateralized glenosphere) was almost twice as much as compared with 25 mm deltoid lengthening. Although below the level required for acute fracture of cortical bone,[3] the observed strain values are high enough to generate microscopic damage (microdamage) possibly leading to fatigue/stress fractures over time. This may be particularly true in patients with low bone density as studies show osteoporosis to be a risk factor for acromial fatigue fractures.[17,28] Our data may help surgeons identify a high-risk population.

Our study is the first to quantify acromial and SS strain patterns in relation to deltoid lengthening. Biomechanical studies using strain gauges on lower extremities demonstrate that above approximately 1500-2500 με, bone undergoes a damage-sensitive transition from linear viscoelasticity.[19] Correspondingly, Schaffler et al[21,22] suggested that cyclic loading at lower strain magnitudes causes microdamage and an associated bony modulus decrease. Beyond these effective strain ranges, bone exhibits small but quantifiable increases in cyclic energy dissipation and decreases in modulus due to prior damage accrual.[19] This finding may have implications for skeletal response to increased chronic loadings such as those seen after RSA. Although Walch et al[25] demonstrated no association of preoperative acromial pathology with clinical outcomes (in terms of postoperative range of motion, Constant score, or subjective results) compared with patients without acromial pathology, it is unknown how acetabularization of the acromion (as seen in Hamada Stage III or IV Cuff tear arthropathy) affects bone density. Existing microdamage can be further susceptible to propagation of damage

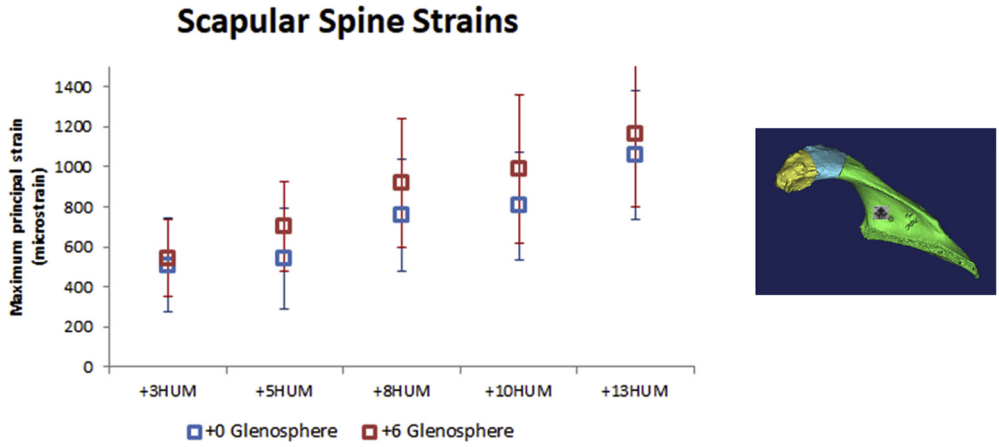

Figure 5 Maximum principal strain on the scapular spine with different implant configurations. At humeral onlay polyethylene thickness above 8 mm, the strain patterns appear to be less linear with both the standard glenosphere and +6 mm lateralized glenosphere.

and failure when exposed to brief episodes of high strain loading.[21,22]

Multiple clinical studies have used radiographic measurements of arm lengthening as a surrogate for deltoid lengthening suggesting a correlation of arm lengthening with increased Constant scores as well as increased internal rotation and anterior forward elevation in RSA.[12,27] Jobin et al[12] reported deltoid lengthening (average 21 mm) correlated with superior active forward elevation and an acromion-greater tuberosity distance exceeding 38 mm had a 90% positive predictive value of obtaining 135° of active forward elevation. Werner et al[27] observed decreases in active anterior elevation and Constant scores in a patient with arm lengthening of more than 25 mm. This may be a critical value for surgeons to bear in mind as there was an 82.6% increase in acromial strain at the maximum deltoid lengthening compared with 25 mm lengthening ($P = .021$). Furthermore, there was a maximal principal strain increase of 79 με/mm (acromion) and 66 με/mm (SS) deltoid lengthening above a threshold of 25 mm.

Our study demonstrated that anatomic variations of the acromion and SS in the parasagittal plane affected strain patterns after RSA. Half of the specimens (group A) showed significantly higher strain on the SS compared with the acromion, regardless of the implant configuration that was tested. The bony anatomy of those 5 specimens (group A) demonstrated a larger mean SSA compared with the other half (group B). The larger SSA indicated a flatter SS relative to the scapular plane. This finding combined with a posteriorly oriented acromion relative to the scapular plane may indicate that as the acromion is more posteriorly oriented, the SS takes on more strain from the deltoid vs. the acromion. Conversely, an anteriorly oriented acromion may confer increased strain on the acromion vs. the SS. An association of strain tendencies with bony anatomy may be valuable for surgeons while using RSA.

The proposed clinical risk factors for AF and SSF include osteoporosis,[17,28] a smaller lateral offset of the greater tuberosity,[28] lateralized glenosphere design,[29] onlay humeral component,[2] Delta angle,[23] and increased arm lengthening.[28] However, there are a few studies that have reported no correlation between the amount of arm lengthening and the risks of post-RSA acromial fractures.[6,12] Also, excessive medialization may create a lower deltoid wrapping angle leading to a more vertical line of pull from the deltoid producing an increased bending moment arm applied to the acromion, further placing the acromion at risk for fracture. In these cases, the greater tuberosity cannot act as a pulley of reflection for the deltoid anymore.[28] Consensus is lacking regarding the etiology of AF and SSFs after RSA. Considering the difficulty in management of these fractures, improved knowledge of strain patterns at the acromion and SS with regard to deltoid lengthening and anatomic variation may be helpful.

The limitations of this study include those inherent with biomechanical cadaveric models including cadaveric acromions vs. cuff tear arthropathy patient acromions that may have more deteriorated bone quality and wear patterns. Furthermore, bone density is a possible confounder especially in pathologic shoulders. However, our specimens were healthy nonarthritic. In addition, deltoid lengthening data from our study may not correlate with the clinical radiographic based studies. However, radiographic measurements as surrogates for deltoid lengthening have a self-reported large SD (−23 to 52 mm).[27] Radiographic arm lengthening may not be the most accurate surrogate for deltoid lengthening and is dependent on multiple factors.[14] The calculation of deltoid lengthening in our study may be a more accurate delineation as the simulation of 5 deltoid fibers more accurately follows the line of action of the deltoid. Furthermore, strain was only measured on the surface of the outer cortex of the acromion and the SS; thus the strains in the deep cortical and trabecular bone may be different. It should be acknowledged that possibly digitizing the implants with the optical tracker may have improved the reliability of the post-virtual implant

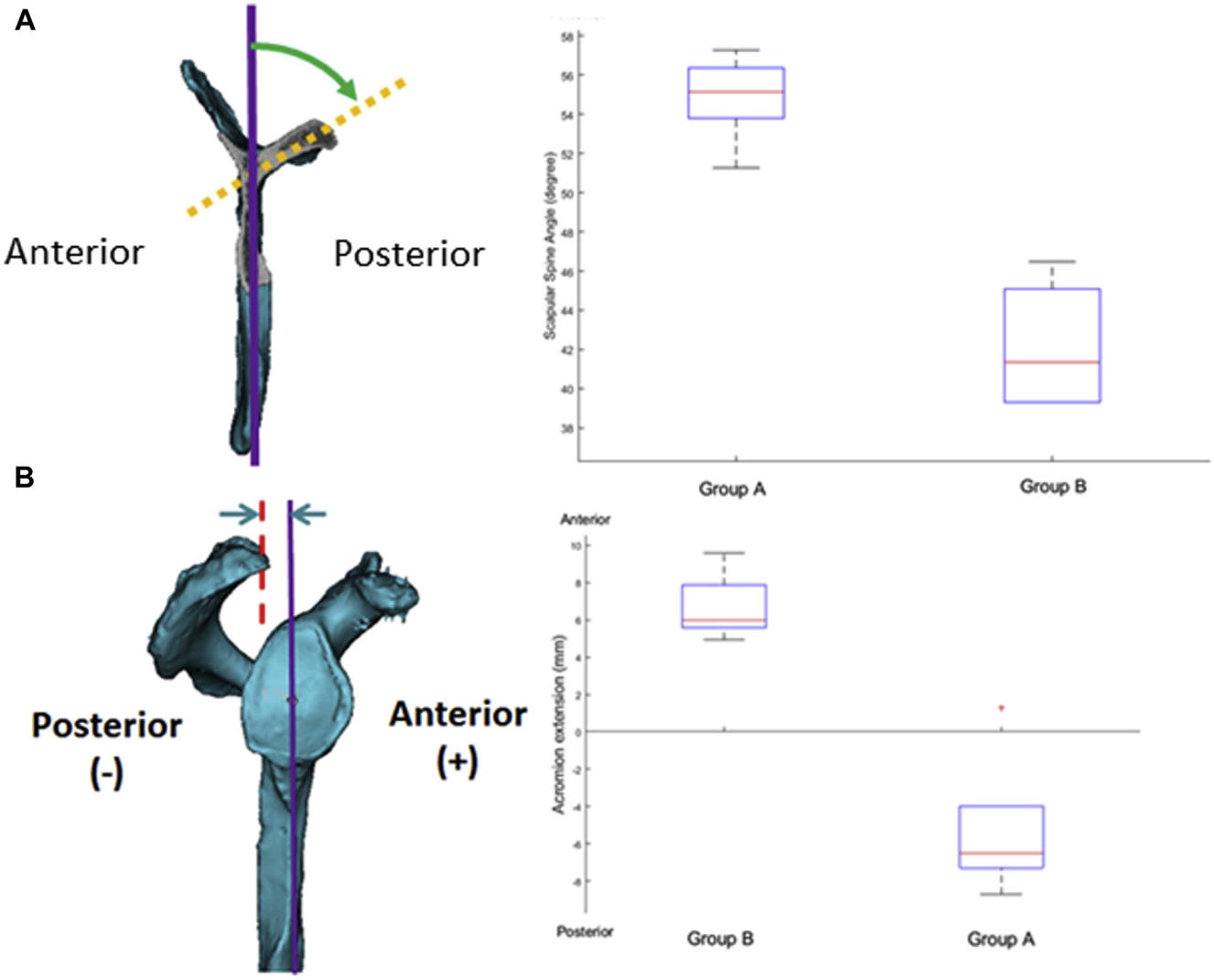

Figure 6 Anatomic variance with regard to the (**A**) scapular spine angle (SSA) and (**B**) position of the acromion. Group A specimen had a larger mean SSA compared with group B (55° vs. 42°; $P < .001$) and had a posteriorly oriented acromion (−5.3 mm, relative to the scapular plane), whereas group B had an anteriorly oriented acromion (6.7 mm, $P < .001$). Group A = significantly higher strain on the scapular spine vs. acromion and group B = significantly higher strain on the acromion vs. scapular spine at maximum deltoid lengthening in adduction.

implantation in the CT model. However, the difference between digitization and our methodology of fitting the shape of central peg and part of the reamed surface is relatively small (approximately 1-2 mm). Furthermore, although adding +3 glenosphere lateralization may add clinical value, the decision was made to use 0 and +6 lateralized center of rotation (COR) glenosphere for the most efficient comparison. The decision was based on a desire for direct comparisons of medialized vs. lateralized COR, as defined by Routman et al,[20] who stated that a glenosphere with a COR of ≤5 mm to the glenoid face is considered a medialized glenoid and a glenosphere with a COR >5 mm lateral to the glenoid face is considered a lateralized glenoid. Also, we measured the most anterior point of the acromion in the parasagittal plane relative to the scapular plane; we did not have any 3D measurements, which would have been more accurate. Furthermore, for reproducibility of the surgical technique, a concentric glenosphere was used as the implant system used in this study allows a range of magnitude and direction of eccentricity. This is a limitation as it may not accurately portray clinical practice and potential other factors leading to arm lengthening. Finally, we did not investigate acromial strains during simulated functional loads, which may further increase strain values. A recent finite element modeling study investigated the effect of RSA implant configuration on acromial stresses during active abduction.[29] The authors reported a 17.2% increase in peak acromial stress from a standard (no lateralization) to 10 mm lateralized glenosphere, as well as a 1.4% increase in peak acromial strain with 5 mm humeral lateralization.[29] However, the authors did not take into account the effect of passive deltoid

tension in their study. Also, the influence of other previously described coronal acromial/scapular parameters (eg, acromion index, critical shoulder angle, etc.) on strain patterns was not examined. However, the SSA and parasagittal orientation of the acromion were selected as simple tools that a surgeon could use during preoperative 3D planning. Further potential limitations are influence of 3D scapular morphology, deltoid segmentation influence on wrapping in rigid body analysis, and a validated simple computer model that may not be a realistic volumetric representation of real muscle. Future studies modeling both passive and active deltoid loads may provide the most insight into the effect of RSA implant configuration on the risks of acromial fractures.

Conclusion

Implant design such as humeral lateralization and glenosphere lateralization resulting in deltoid lengthening significantly increases strains on the acromion and SS after RSA, particularly with deltoid lengthening above 25 mm. Anatomic variation may indicate that as the acromion is more posteriorly oriented, the SS takes more strain from the deltoid vs. the acromion. Our study's data may help surgeons identify a high-risk population for increased strain patterns after RSA.

Disclaimer

The other authors, their immediate families, and any research foundations with which they are affiliated have not received any financial payments or other benefits from any commercial entity related to the subject of this article.

References

1. Ackland DC, Roshan-Zamir S, Richardson M, Pandy MG. Moment arms of the shoulder musculature after reverse total shoulder arthroplasty. J Bone Joint Surg Am 2010;92:1221-30. https://doi.org/10.2106/JBJS.I.00001
2. Ascione F, Kilian CM, Laughlin MS, Bugelli G, Domos P, Neyton L, et al. Increased scapular spine fractures after reverse shoulder arthroplasty with a humeral onlay short stem: an analysis of 485 consecutive cases. J Shoulder Elbow Surg 2018;27:2183-90. https://doi.org/10.1016/j.jse.2018.06.007
3. Bayraktar HH, Morgan EF, Niebur GL, Morris GE, Wong EK, Keaveny TM. Comparison of the elastic and yield properties of human femoral trabecular and cortical bone tissue. J Biomech 2004;37:27-35. https://doi.org/10.1016/s0021-9290(03)00257-4
4. Charlton IW, Johnson GR. A model for the prediction of the forces at the glenohumeral joint. Proc Inst Mech Eng H 2006;220:801-12. https://doi.org/10.1243/09544119JEIM147
5. Crosby LA, Hamilton A, Twiss T. Scapula fractures after reverse total shoulder arthroplasty: classification and treatment. Clin Orthop Relat Res 2011;469:2544-9. https://doi.org/10.1007/s11999-011-1881-3
6. Dubrow S, Streit JJ, Muh S, Shishani Y, Gobezie R. Acromial stress fractures: correlation with acromioclavicular osteoarthritis and acromiohumeral distance. Orthopedics 2014;37:e1074-9. https://doi.org/10.3928/01477447-20141124-54
7. Farshad M, Gerber C. Reverse total shoulder arthroplasty-from the most to the least common complication. Int Orthop 2010;34:1075-82. https://doi.org/10.1007/s00264-010-1125-2
8. Garner BA, Pandy MG. The obstacle-set method for representing muscle paths in musculoskeletal models. Comput Methods Biomech Biomed Engin 2000;3:1-30.
9. Garner BA, Pandy MG. Musculoskeletal model of the upper limb based on the visible human male dataset. Comput Methods Biomech Biomed Engin 2001;4:93-126.
10. Giles JW, Langohr GD, Johnson JA, Athwal GS. Implant design variations in reverse total shoulder arthroplasty influence the required deltoid force and resultant joint load. Clin Orthop Relat Res 2015;473:3615-26. https://doi.org/10.1007/s11999-015-4526-0
11. Henninger HB, Barg A, Anderson AE, Bachus KN, Burks RT, Tashjian RZ. Effect of lateral offset center of rotation in reverse total shoulder arthroplasty: a biomechanical study. J Shoulder Elbow Surg 2012;21:1128-35. https://doi.org/10.1016/j.jse.2011.07.034
12. Jobin CM, Brown GD, Bahu MJ, Gardner TR, Bigliani LU, Levine WN, et al. Reverse total shoulder arthroplasty for cuff tear arthropathy: the clinical effect of deltoid lengthening and center of rotation medialization. J Shoulder Elbow Surg 2012;21:1269-77. https://doi.org/10.1016/j.jse.2011.08.049
13. Levy JC, Anderson C, Samson A. Classification of postoperative acromial fractures following reverse shoulder arthroplasty. J Bone Joint Surg Am 2013;95:e104. https://doi.org/10.2106/JBJS.K.01516
14. Lädermann A, Edwards TB, Walch G. Arm lengthening after reverse shoulder arthroplasty: a review. Int Orthop 2014;38:991-1000. https://doi.org/10.1007/s00264-013-2175-z
15. Mayne IP, Bell SN, Wright W, Coghlan JA. Acromial and scapular spine fractures after reverse total shoulder arthroplasty. Shoulder Elbow 2016;8:90-100. https://doi.org/10.1177/1758573216628783
16. Neyton L, Erickson J, Ascione F, Bugelli G, Lunini E, Walch G. Grammont Award 2018: Scapular fractures in reverse shoulder arthroplasty (Grammont style): prevalence, functional, and radiographic results with minimum 5-year follow-up. J Shoulder Elbow Surg 2019;28:260-7. https://doi.org/10.1016/j.jse.2018.07.004
17. Otto RJ, Virani NA, Levy JC, Nigro PT, Cuff DJ, Frankle MA. Scapular fractures after reverse shoulder arthroplasty: evaluation of risk factors and the reliability of a proposed classification. J Shoulder Elbow Surg 2013;22:1514-21. https://doi.org/10.1016/j.jse.2013.02.007
18. Patterson DC, Chi D, Parsons BO, Cagle PJ. Acromial spine fracture after reverse total shoulder arthroplasty: a systematic review. J Shoulder Elbow Surg 2019;28:792-801. https://doi.org/10.1016/j.jse.2018.08.033
19. Pattin CA, Caler WE, Carter DR. Cyclic mechanical property degradation during fatigue loading of cortical bone. J Biomech 1996;29:69-79.
20. Routman HD, Flurin PH, Wright TW, Zuckerman JD, Hamilton MA, Roche CP. Reverse shoulder arthroplasty prosthesis design classification system. Bull Hosp Jt Dis (2013) 2015;73(Suppl 1):S5-14.
21. Schaffler MB, Radin EL, Burr DB. Mechanical and morphological effects of strain rate on fatigue of compact bone. Bone 1989;10:207-14.
22. Schaffler MB, Radin EL, Burr DB. Long-term fatigue behavior of compact bone at low strain magnitude and rate. Bone 1990;11:321-6.
23. Schenk P, Aichmair A, Beeler S, Ernstbrunner L, Meyer DC, Gerber C. Acromial fractures following reverse total shoulder arthroplasty: a cohort controlled analysis. Orthopedics 2020;43:15-22. https://doi.org/10.3928/01477447-20191031-03
24. Teusink MJ, Otto RJ, Cottrell BJ, Frankle MA. What is the effect of postoperative scapular fracture on outcomes of reverse shoulder arthroplasty? J Shoulder Elbow Surg 2014;23:782-90. https://doi.org/10.1016/j.jse.2013.09.010

25. Walch G, Mottier F, Wall B, Boileau P, Molé D, Favard L. Acromial insufficiency in reverse shoulder arthroplasties. J Shoulder Elbow Surg 2009;18:495-502. https://doi.org/10.1016/j.jse.2008.12.002
26. Werner BC, Chen X, Camp CL, Kontaxis A, Dines JS, Gulotta LV. Medial posterior capsular plication reduces anterior shoulder instability similar to remplissage without restricting motion in the setting of an engaging Hill-Sachs defect. Am J Sports Med 2017;45:1982-9. https://doi.org/10.1177/0363546517700860
27. Werner BS, Ascione F, Bugelli G, Walch G. Does arm lengthening affect the functional outcome in onlay reverse shoulder arthroplasty? J Shoulder Elbow Surg 2017;26:2152-7. https://doi.org/10.1016/j.jse.2017.05.021
28. Werthel J-D, Schoch BS, van Veen SC, Elhassan BT, An K-N, Cofield RH, et al. Acromial fractures in reverse shoulder arthroplasty: a clinical and radiographic analysis. J Shoulder Elbow Arthroplasty 2018;2:2471549218777628. https://doi.org/10.1177/2471549218777628.
29. Wong MT, Langohr GDG, Athwal GS, Johnson JA. Implant positioning in reverse shoulder arthroplasty has an impact on acromial stresses. J Shoulder Elbow Surg 2016;25:1889-95. https://doi.org/10.1016/j.jse.2016.04.011